An Overview of Real-Time WRF Testing at NCEP

Matthew E. Pyle[1], Zavisa Janjic, Tom Black and Brad Ferrier[1]
National Centers for Environmental Prediction, Camp Springs, MD
[1] and Science Applications International Corporation (SAIC)

1. INTRODUCTION

Real-time testing of both the NCEP (WRF-NMM) and NCAR (WRF-MC) developed WRF dynamical cores has been ongoing at NCEP since November 2003. These runs are being made to prepare NCEP for the scheduled implementation of a WRF system into the operational modeling suite in October 2004. This paper reviews NCEP's real-time WRF modeling activity.

A brief introduction to the horizontal and vertical structure of the WRF-NMM will be provided, as each differs from what is used in the WRF-MC. However, differences in the dynamics of the WRF-NMM and WRF-MC are beyond the scope of this paper. Details of the real-time system, including domain specification, physics options, and the flow of data through the system, also will be described. Finally, a brief review of the quantitative statistics generated for each of the models over a multi-month period is given, followed by a short description of current work.

2. INITIALIZATION OF THE WRF-NMM

WRF-NMM runs at NCEP are initialized through the same basic mechanism as the WRF-MC runs: the standard initialization (SI) reads GRIB data from an initializing model and interpolates it onto the target WRF domain grid. However, the functionality of the SI had to be expanded to handle the horizontal staggering, map projection, and vertical coordinate used by the WRF-NMM, as each is distinct from its WRF-MC counterpart.

The WRF-NMM uses an Arakawa E grid (e.g., Arakawa and Lamb 1977; Black 1994, Fig. 2), where both wind components are collocated on the same grid point offset from the associated mass point. Rationale for selecting an E grid over the more widely used Arakawa C grid is discussed elsewhere (e.g., Black 1994), and in the interest of brevity the discussion will not be repeated here.

Another key difference between the WRF-NMM and WRF-MC relevant to model initialization is the use of a rotated latitude-longitude grid in the WRF-NMM. The simplicity of a latitude-longitude grid is made applicable over the entire globe by rotating the earth's latitude-longitude grid such that the equator and prime meridian intersect at the center of the WRF-NMM's computational grid. This rotation minimizes the convergence of meridians, keeping the true horizontal scale relatively uniform over the domain.

The final WRF-NMM characteristic incorporated into the SI is the hybrid pressure-sigma vertical coordinate. WRF-NMM model surfaces are terrain-following sigma surfaces near the ground, purely isobaric above a prescribed pressure value (typically about 420 hPa), and relax from terrain following to isobaric over the intervening depth. Further details of the vertical coordinate can be found in Janjic (2003).

3. THE REAL-TIME SYSTEM

The four large test domains used for WRF-NMM and WRF-MC real-time test runs are depicted in Figure 1. Both models generate a 48 h forecast once per day for each region on the following schedule: Alaska (00Z); West (06Z); Central (12Z); East (18Z). These model domains also were used for the recently completed WRF Developmental Testbed Center (DTC) retrospective runs. The WRF-NMM at NCEP is run with 8 km horizontal grid spacing and 60 vertical levels, while the WRF-MC is run with 10 km horizontal grid spacing and 50 vertical levels. This discrepancy in resolution results from a desire to better balance the computer resources required to run each model, and

FIG.1. The four large real-time WRF test domains used at NCEP for both the WRF-NMM and WRF-MC models.

Corresponding author address: Matthew Pyle, NCEP/EMC, 5200 Auth Road, Room 204, Camp Springs, MD 20746. Matthew.Pyle@noaa.gov

matches the resolutions used for each model in the DTC retrospective runs. Another difference in the configuration of each model is that the WRF-MC uses a filtered topography, while the WRF-NMM topography is unsmoothed except for the outermost rows of the domain.

Table 1 summarizes the physics options used for each model run. Each model is configured like its control run from the DTC retrospective testing. Due to the use of different physics packages, forecast differences between the two models result both from differences in physics as well as the core dynamics.

All domains are initialized from Eta model forecast GRIB data for both the WRF-NMM and WRF-MC. Both models thus have a common starting point, and avoid a potential source of difference.

WRF-NMM	WRF-MC
Ferrier microphysics	Ferrier microphysics
Betts-Miller-Janjic convection	Kain-Fritsch convection
Mellor-Yamada-Janjic PBL	YSU PBL
GFDL shortwave radiation	Dudhia shortwave radiation
GFDL longwave radiation	RRTM longwave radiation
NOAH land surface model	NOAH land surface model

TABLE 1. The physics options used in the NCEP real-time runs.

Output from each model is postprocessed to bring them back to a common format that enables direct comparison. The NCEP WRF postprocessor vertically interpolates output from each model onto isobaric surfaces, diagnoses various fields not directly computed by the models, and generates a GRIB file on the model's native projection (rotated latitude longitude for the WRF-NMM and Lambert Conformal for the WRF-MC). NCEP's "product generator" horizontally interpolates the data from each model onto a common grid used for visualization and verification.

4. DISCUSSION OF VERIFICATION RESULTS

Quantitative verification statistics have been generated for the real-time WRF run at NCEP since both cores began running routinely.With four domains, two models, and approximately six months of verification data to examine, an effort to focus the discussion is made by limiting most discussion to the January 2004 through March 2004 period, and to the three CONUS domains.

The surface and upper-air statistics are computed by comparison of a model forecast value interpolated to the location of a specific observation. All upper-level statistics are based on verification against radiosonde data only.

The overall impression from the verification of upper-air fields such as temperature, geopotential height, winds and relative humidity is that they are relatively similar to one another and to NCEP's operational NMM, which runs over the same regions as the WRF runs and serves as a non-WRF benchmark. It is important to keep in mind that the WRF-NMM was an experimental model over this period, and that test changes to dynamics and physics are reflected in the scores. The operational NMM verification statistics are one gauge of that model's present level of skill, and represent the minimum level of skill sought in current efforts to improve the WRF-NMM.

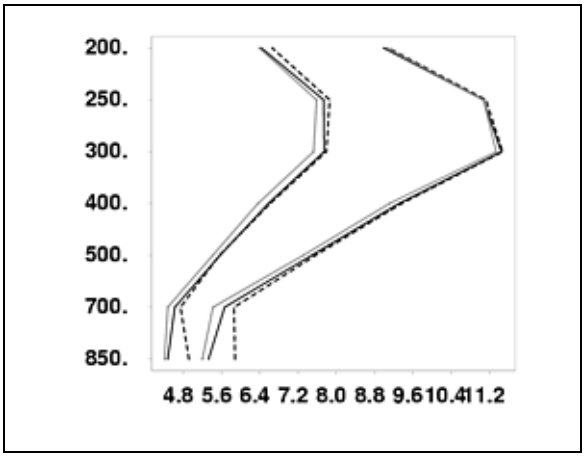

FIG. 2. The vertical profile of RMS wind errors (m s^{-1}) for the western domain for January-March 2004 for: WRF-NMM (solid black), WRF-MC (dashed), and operational NMM (solid gray). The left set of curves represents the 18 h forecast, while the right set of curves depicts the 42 h forecast.

Temperature and wind were the two fields for which the upper-level verifications were most similar to each another over the three CONUS domains. The western domain RMS wind errors (Fig. 2) are very similar above 700 hPa in both WRF over the January-March 2004 period. The central domain temperature errors (Fig. 3) show slightly more variation, with smaller errors for the WRF-NMM at lower levels, and larger errors above 500 hPa.

An upper-level field showing somewhat more difference was geopotential height, as the WRF-MC generally had lower height errors than the WRF-NMM over the January-March period, particularly for shorter forecast ranges and at upper levels. The SI of the WRF-NMM had a small flaw that generated an upper-

level warm bias and a resulting height bias in upper-level geopotential height fields in the WRF-NMM until corrected in mid-March 2004. Results from May 2004, after the SI problem had been fixed, look considerably different with the WRF-NMM generally having lower height errors than the WRF-MC for the western and eastern domains, and with both models having similar height errors for the central domain.

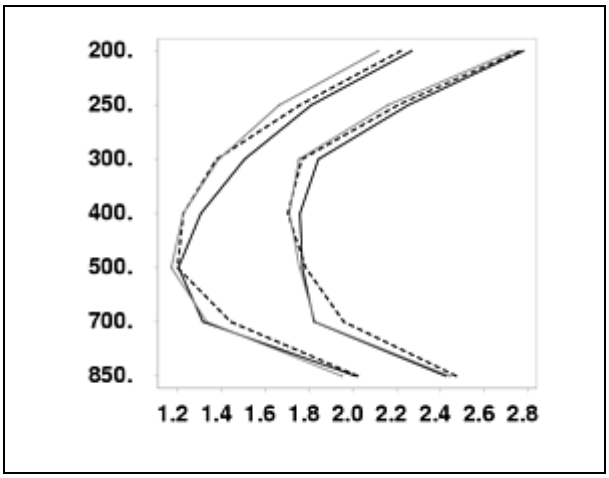

FIG. 3. As in Fig. 2, except for RMS temperature errors (°C) for the central domain, and for 24 h and 48 h forecasts.

Relative humidity statistics varied somewhat from region to region, with the WRF-MC showing lower errors for the central and eastern domains. Relative humidity statistics for the western and Alaskan domains were very similar between the models.

Shelter (2m) temperature forecasts were analyzed separately for forecast hours surrounding the afternoon temperature maximum and early morning temperature minimum. For the three CONUS domains examined over the January-March 2004 period, the WRF-NMM demonstrated a daytime warm bias and a nighttime cool bias. The WRF-MC had exactly the opposite signal, with a daytime cool bias and nighttime warm bias. Thus the WRF-NMM forecasts a larger than observed diurnal temperature variation, while the WRF-MC depicts a smaller than observed diurnal cycle. While the bias was significantly different in each model, the RMS errors averaged over the domains were fairly similar for the WRF-NMM (averaging 3.6°C for the daytime maximum/ 3.7°C for the nighttime minimum) and the WRF-MC (3.4°C/ 3.5°C).

This shelter temperature bias signal was largest over the western domain, with Fig. 4 showing a scatter plot of daytime temperature bias for each model. The WRF-NMM has an average daytime warm bias for this period of 0.8°C, while the WRF-MC has an average cool bias of 1.1°C. The nighttime temperature bias is depicted in Fig. 5, and once again there is a distinct difference with the WRF-NMM averaging a nighttime cool bias of 1.2°C and the WRF-MC having an average warm bias of 1.2°C.

Surface (10 m) wind forecasts also show significant differences between the two models over all three CONUS domains. The WRF-NMM had a low bias in surface wind speed, while the WRF-MC had a high wind speed bias over the three regions. In addition to these different bias characteristics, the WRF-NMM shows significantly lower (3.0 m s^{-1}) RMS wind errors than the WRF-MC (3.8 m s^{-1}) in an average over the three CONUS domains for January-March 2004. A scatter plot of western domain surface wind RMS errors is shown in Fig. 6; for this domain the WRF-NMM has an average RMS error of 3.5 m s^{-1} while the WRF-MC has an average RMS error of 4.5 m s^{-1}.

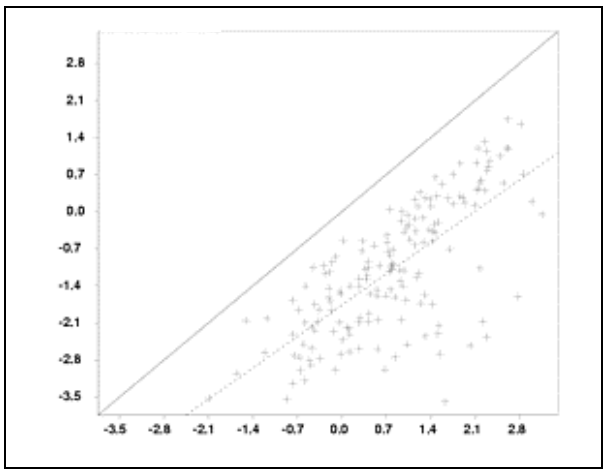

FIG. 4. A scatter plot of 2 m temperature bias over the western domain for late afternoon (21Z and 00Z valid times). The WRF-NMM values are depicted along the x-axis, and the WRF-MC values are provided on the y-axis. Forecasts less than 12 h into the integration were not considered. The solid diagonal line denotes where the bias is equivalent in each model.

Precipitation verifications for 24 h accumulations show considerable variation from month to month and between the three CONUS domains. Over the January-March 2004 period, the WRF-MC demonstrated generally higher equitable threat scores (Schaeffer 1990) for both the central and eastern domains, while the WRF-NMM was slightly better over the western domain. The Betts-Miller-Janjic (BMJ) convective parameterization in the WRF-NMM was undergoing testing and significant revisions in the real-time runs over this period, so these precipitation verifications should be considered preliminary. The current real-time WRF-NMM is considerably different as a precipitation forecast model than it was between January and March 2004.

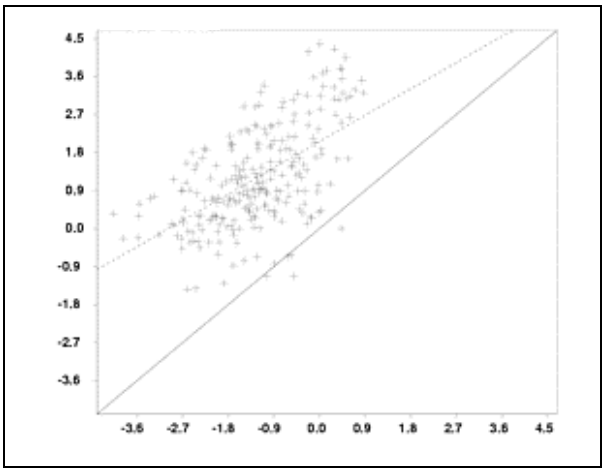

FIG. 5. As in Fig. 4, but for late night hours (forecast valid times between 09Z and 15Z).

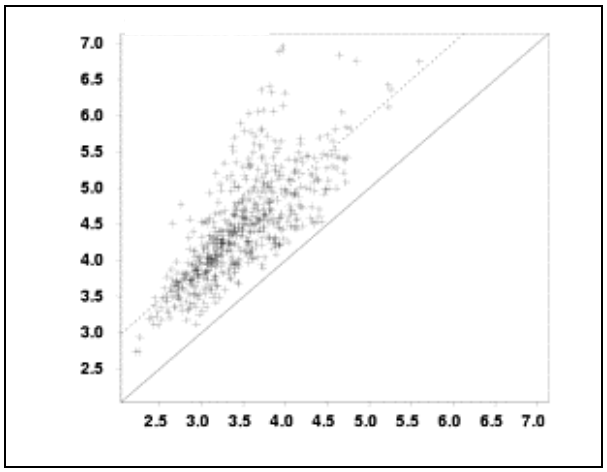

FIG. 6. A scatter plot of 10 m wind RMS errors (m s^{-1}) for the western domain over the January-March 2004 period. The WRF-NMM values are depicted along the x-axis, and the WRF-MC values are provided on the y-axis. All forecast hours are included in the verification. The solid diagonal line denotes where the RMS error is equivalent in each model.

5. CURRENT WORK AND FUTURE PLANS

The most active region of WRF work at NCEP, aside from preparing a WRF system for operational implementation in fall 2004, is continued refinement of the physics package used with the WRF-NMM. In particular, the BMJ convective parameterization has been undergoing revision to better capture heavy precipitation bands while keeping precipitation bias under control. Initial results have shown promise in improving the WRF-NMM's quantitative precipitation forecast skill, but these changes need more testing over a longer period before more definitive conclusions can be reached.

6. REFERENCES

Arakawa, A., and V. R. Lamb, 1977: Computational design of the basic dynamical processes of the UCLA general circulation model. *Methods Comput. Phys*., **17**, 173-265.

Black, T. L., 1994: The New NMC Mesoscale Eta model: Description and forecast examples. *Wea. Forecasting*., **9**, 265-278.

Janjic, Z. I., 2003: A Nonhydrostatic Model Based on a New Approach. *Meteorol. Atmos. Phys*., **82**, 271-285.

Schaefer, J.T., 1990: The critical success index as an indicator of warning skill. *Wea. Forecasting*., **5**, 570-575.